Bioactive Materials 2 (2017) 162–169

Contents lists available at ScienceDirect

Bioactive Materials

journal homepage: http://www.keaipublishing.com/en/journals/bioactive-materials/

High velocity suspension flame spraying (HVSFS) of metal doped bioceramic coatings

P. Krieg [a, *], A. Killinger [a], R. Gadow [a], S. Burtscher [b], A. Bernstein [b]

[a] Institute for Manufacturing Technologies of Ceramic Components and Composites (IMTCCC), University of Stuttgart, Allmandring 7b, 70569 Stuttgart, Germany

[b] Musculoskeletal Research Lab, Department of Surgery, Clinics of Orthopedics and Trauma Surgery, University of Freiburg – Medical Centre, Hugstetter Straße 55, 79106 Freiburg, Germany

ARTICLE INFO

Article history:
Received 28 February 2017
Received in revised form
19 April 2017
Accepted 21 April 2017
Available online 2 May 2017

1. Introduction

Calcium phosphate ceramics, such as hydroxyapatite or tricalciumphosphate as well as bioglass, are successfully used as coatings to improve the fixation of dental implants or load-bearing implants in the human bone [1]. The demand for surgical procedures such as hip and knee arthroplasties, primary as well as revision procedures, is projected to increase for the foreseeable future [2]. The possibility of an infection is a major risk for all implants [3]. The treatment of these periprosthetic joint infections is difficult and often requires the replacement of the implant [4], which is a significant burden for the patient and comes at an increased economic cost [5].

A possible approach to this problem is the use of an antibacterial coating, which should promote the attachment of the implant to the bone while reducing the risk of inflammation. In this study, three different metals with known antibacterial properties are combined with four different bioceramic materials to produce such coatings. The metals used for their antibacterial properties are silver [6–8], bismuth [9] and copper [10,11]. The coatings are deposited using high velocity suspension flame spraying (HVSFS). Thermal spraying [18] of bioceramic coatings is an established procedure, especially the deposition by plasma spraying [19–22]. While the HVSFS is a comparatively new process, the deposition of bioceramic coatings has already been investigated [12–16]. The HVSFS allows for the manufacturing of thin coatings with coating thicknesses in the range of 15–50 μm. Thermally sprayed coatings with that coating thickness can lead to advantageous mechanical properties, such as a reduced risk of delamination during crack formation [17].

2. Materials and methods

2.1. Preparation of the ceramic suspensions

Four different feedstock powders were employed in this study: hydroxyapatite (HA) [23,24] ($Ca_{10}(PO_4)_6(OH)_2$; Ceram GmbH, Germany), beta-tricalciumphosphate (TCP) ($Ca_3(PO_4)_2$; Budenheim, Germany), a calcium potassium sodium phosphate, GB14 [25], with the main crystalline phase $Ca_2KNa(PO_4)_2$ (BAM, Germany) and a bioglass (BG) with a composition of 47.3% SiO_2, 28.6% CaO, 15.2% P_2O_5, 4.90% Na_2O, 2.50% MgO and 1.5% F (Colorobbia, Italy).

To obtain suspensions suitable for the HVSFS process, these powders were dispersed in water, isopropanol, ethanol or a mixture thereof, depending on their individual properties. All suspensions were prepared with a solid content of 10 wt-% and were milled in an attrition mill using zirconia milling balls with a diameter of 2–2.5 mm and, to prevent sedimentation, stabilized using an alkyl phosphate dispersing additive for the isopropanol and ethanol based suspensions (KV9067, Zschimmer & Schwarz, Germany) and Dolapix CE 64 (Zschimmer & Schwarz GmbH, Germany) for the aqueous suspensions.

An overview of the particle sizes, measured by laser diffraction technique (Mastersizer 3000, Malvern Instruments, Malvern, UK) is given in Table 1.

In order to achieve antibacterial properties of the coatings, three metals or metal compounds with known antibacterial properties were added to the suspensions: a soluble silver salt (silver nitrate), a soluble copper salt (copper acetate monohydrate) and bismuth particles (all from Alfa Aesar, Germany). Metals were added equal to 1.75 wt.-% based on the content of the bioceramic matrix material.

Coatings of each of the four bioceramic materials combined with

* Corresponding author.
E-mail address: peter.krieg@ifkb.uni-stuttgart.de (P. Krieg).
Peer review under responsibility of KeAi Communications Co., Ltd.

http://dx.doi.org/10.1016/j.bioactmat.2017.04.006

Table 1
Particle size before and after milling.

Powder	Manufacturer	d10 [μm]; before milling	d50 [μm]; before milling	d90 [μm]; before milling	d10 [μm]; after milling	d50 [μm]; after milling	d90 [μm]; after milling
HA	Ceram	1.88 ± 0.05	6.08 ± 0.22	14.26 ± 2.03	0.07 ± 0.00	1.19 ± 0.12	3.81 ± 0.08
TCP	Budenheim	1.47 ± 0.13	3.75 ± 0.01	12.98 ± 0.12	0.08 ± 0.00	0.33 ± 0.01	1.10 ± 0.13
GB14	BAM	2.66 ± 0.01	17.44 ± 0.06	61.00 ± 0.76	0.50 ± 0.07	1.08 ± 0.25	3.48 ± 0.10
Bioglass	Colorobbia	2.98 ± 0.01	8.03 ± 0.02	24.03 ± 0.17	1.07 ± 0.03	3.05 ± 0.04	6.89 ± 0.06

each of the three metals as well as a control sample without metals were produced, meaning that a total of 16 different coatings were investigated.

2.2. Deposition of the coatings

For the HVSFS process, a TopGun-System (GTV GmbH, Luckenbach, Germany) was used. A combustion chamber with a length of 22 mm and a 78 mm long expansion nozzle was mounted on the torch. The suspension was injected axially in the combustion chamber through an injector with a diameter of 0.5 mm. The suspension feeding system consists of a mechanical pump with two distinctive feeding lines, one for the suspension and one for a cleaning fluid. The suspension was constantly kept in motion and continuously stirred during the process to ensure that no sedimentation occurs.

For the preliminary investigation of the coatings and the in vitro characterization, planar grade 2 titanium substrates with a size of 50×50 mm^2 were used. The torch is mounted on a six-axis robot describing a meander movement in front of the substrates with a speed of 500 mm/s. All materials were sprayed at a distance of 110 mm from the torch to the substrate, with the exception of the bioglass, which was sprayed at a distance of 120 mm.

After these investigations, the robot kinematic was adapted to coat the implants for the in vivo investigations. The implants are made of small titanium alloy rods with a diameter of 4 mm and a length of 240 mm which were cut and trimmed at a length of 16 mm from the coated rod. Due to the wide array of possible combinations, in vivo experiments for all material combinations were not possible. As a consequence, only copper doped coatings and non-doped coatings were deposited on the implant geometries.

The deposition occurs in multiple passes of the torch over the substrate depending on the substrate geometry as well as the desired coating thickness. In the case of the flat substrates, the coating was deposited in two passes while the implant geometries required up to 20 passes of the torch due to the small diameter and the curvature of the cylinder.

All substrates were grit blasted (corundum F60, pressure 6 bar) to ensure a proper mechanical adhesion, cleaned with pressurized air and degreased using acetone. While the TopGun-system allows the use of a wide variety of fuel gases, all coatings in this study were sprayed using a non-stoichiometric ethene-oxygen mixture of 210 slpm oxygen and 90 slpm ethene, favoring a fuel rich combustion with the intent of limiting the oxidation of the metals during the spraying process. The spraying parameters should ensure a sufficient melting behavior of the particles without unnecessary thermal impact to avoid thermal degradation of the materials.

A more thorough description of the HVSFS process and setup can be found in Ref. [26].

2.3. Characterization of the coatings

Optical microscopy images were taken using a Leica MEF4M (Leica GmbH, Germany). SEM images of the surface and the EDX mapping of the cross-sections were taken using a field emission gun SEM DSM 982 Gemini (Zeiss AG, Germany). Hardness measurements on the cross-sections were performed with a Fisherscope H100 (Helmut Fischer GmbH & Co., Germany). Due to the coating thickness, the hardness was measured using Vickers hardness 0.01.

The phase composition of the starting powders was investigated using an X'Pert MPD (PANalytical) with a Cu-kα radiation source operating at 40 kV and 40 mA and a PANalytical X'Celerator detector. The phase composition of the implant coatings was measured using a Bruker D8 Discover DaVinci with parallel beam geometry operated at 40 kV and 40 mA for the hydroxyapatite, TCP and GB14 and 30 mA for the bioglass in a 2Θ range from 20 to 60°. The results were evaluated by means of the DiffracPlus Eva software, superimposing the experimental data with data from the software data base.

To evaluate the biocompatibility, a live/dead-assay Viability/Cytotoxicity Assay Kit (Thermo Fisher Scientific, Switzerland) with MG-63 cells over 3, 7, 14 and 21 days was performed and quantified.

3. Results and discussion

3.1. Coating structure

As depicted in Fig. 1 for the metal doped hydroxyapatite, the coatings show a distinctive color depending on the metal incorporated in the suspension. Especially for the copper and silver doped materials, the color differs optically from the typical grayish non-doped coatings, while the bismuth doped systems are closer in

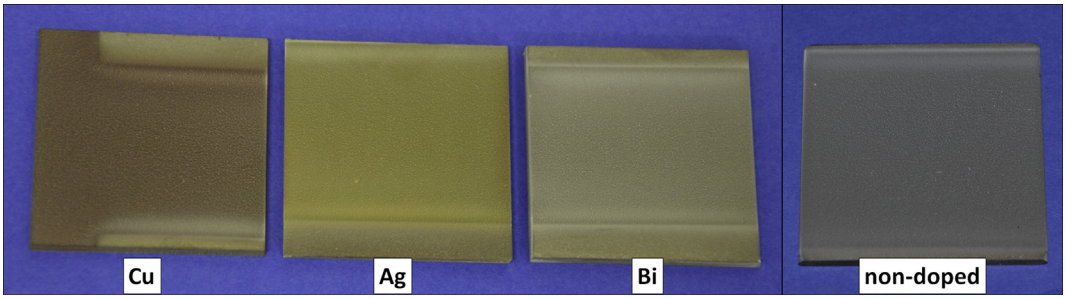

Fig. 1. Hydroxyapatite coatings doped with copper, silver, bismuth and without metal dopant.

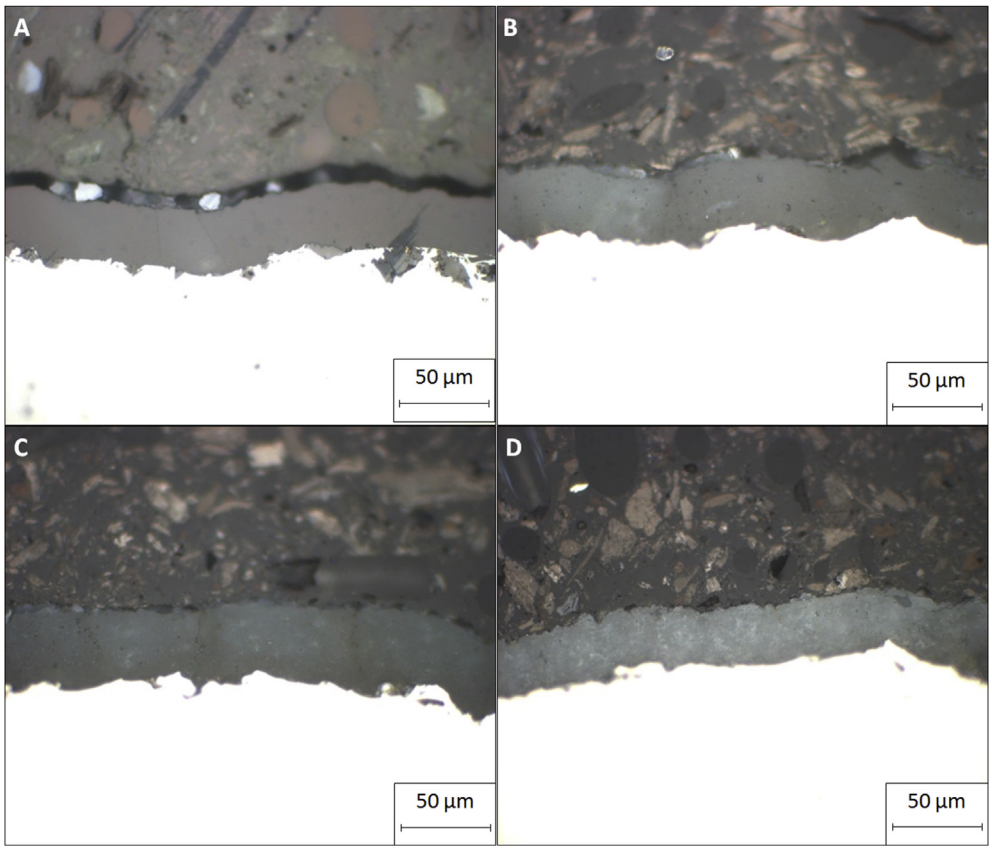

Fig. 2. Cross sections of the non-doped implant coatings; a) hydroxyapatite; b) TCP; c) GB14; d) bioglass.

color to the non-doped coatings.

Fig. 2 shows the micrograph cross-sections of the different bioceramic materials without metal dopant. The micrographs show a dense and homogeneous microstructure for the hydroxyapatite, the TCP and the GB14. For the bioglass, a low level of porosity can be observed. Due to the small diameter of the implant geometry and the dense coating structure, the formation of cracks from the substrate to the coating surface can be observed.

An overview of the coating thickness as well as the roughness for all coatings is shown in Fig. 3. The coatings on the flat titanium substrates show thicknesses between 10 and 25 µm, depending on the bioceramic matrix, with the highest coating thickness for the GB14 and the lowest for the bioglass. This is presumably due to a combination of lower deposition efficiency for the bioglass as well

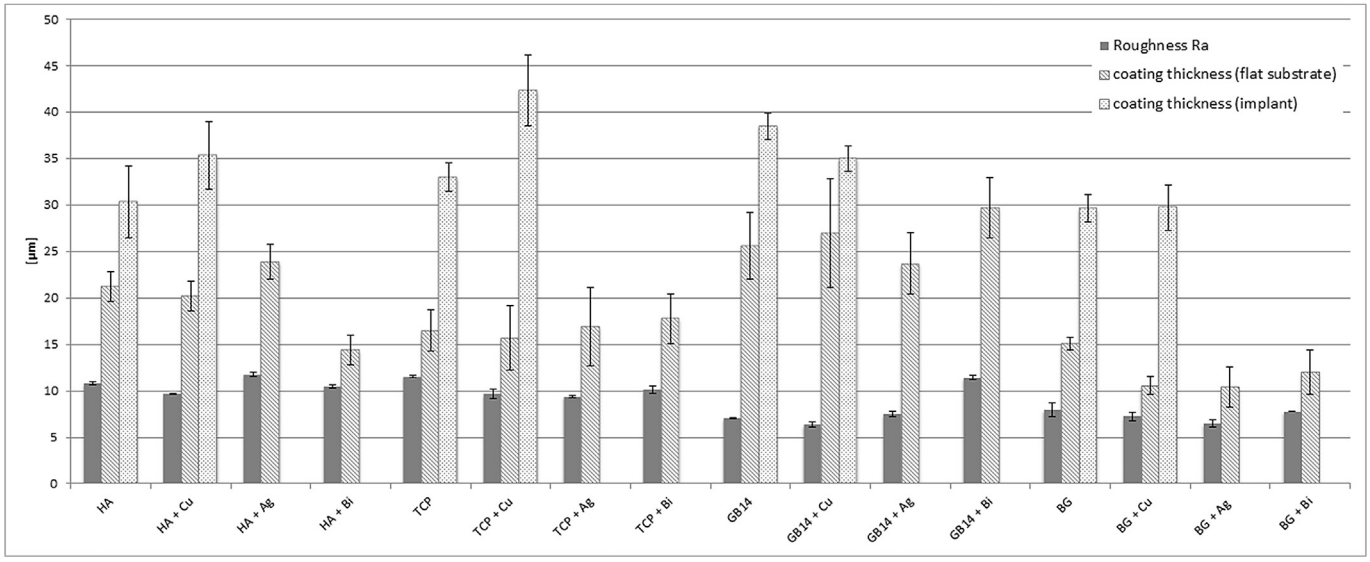

Fig. 3. Roughness and coating thickness for all material combinations.

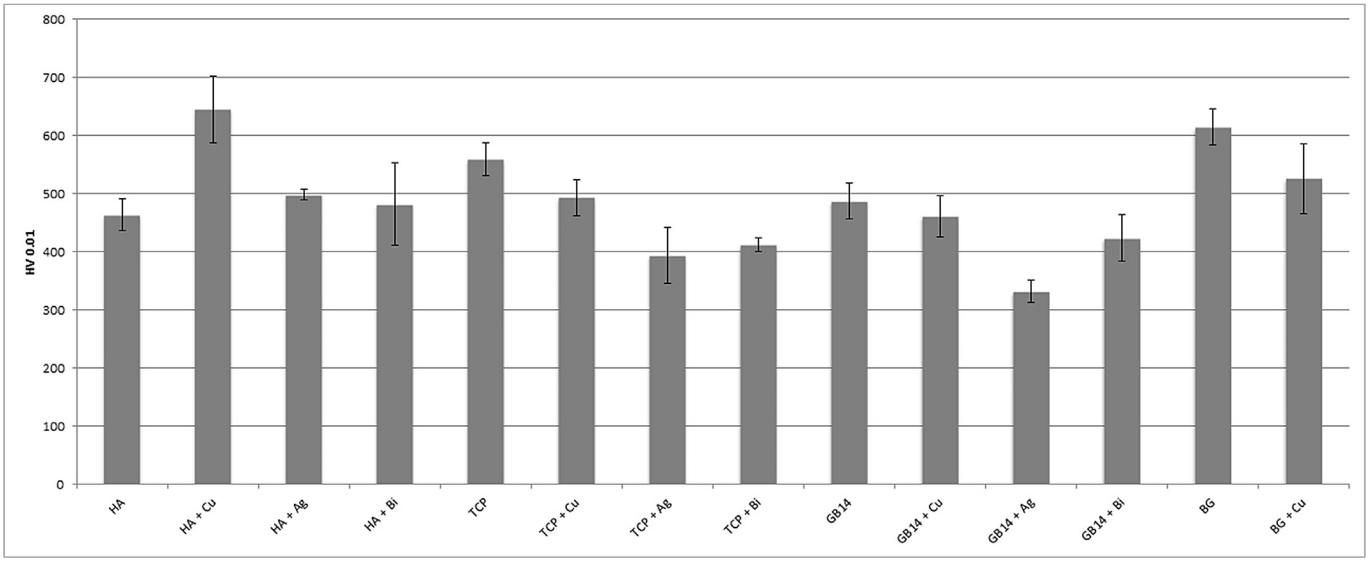

Fig. 4. Vickers hardness HV0.01.

as the slightly higher spraying distance at which the bioglass was sprayed. The coatings on the implants for the in vivo study are in the range between 20 and 50 μm with a homogeneous thickness on the whole circumference.

The addition of the different metal dopants has no significant effect on the mechanical properties of the coatings with one exception: the addition of copper in the hydroxyapatite coating results in an increase in hardness HV0.01 compared to the non-doped hydroxyapatite of about 39%, as shown in Fig. 4. For the other combinations of the different bioceramic materials and copper, silver or bismuth, no comparable trend or effect could be observed. Due to the low coating thickness, the hardness of the bioglass coatings could only be measured on the implant coatings and not the flat substrates. As a result, the data for the silver and bismuth doped bioglass is not available.

Due to the combination of thin coatings and the grit-blasting with coarse corundum F60, the roughness of the implant coatings is comparable to the roughness of the substrate.

Fig. 5 shows a selection of FE-SEM images of the coating surfaces at resolutions between 5,000× and 20,000×. The FE-SEM images show the typical surface structure expected of such thermally sprayed coatings with characteristic splat formation as well as spherically re-solidified particles.

In Fig. 5A)–D), the non-dopped reference coatings are shown for each of the four respective material systems. Due to the similar nature of the materials, especially the calcium phosphates, the microstructure of the surface appears similar. The GB14 coating however, shows a distinctive microroughness on the splats (Fig. 5D)). The crack formation already observerd in the cross-sections can also be observed in the FE-SEM images (Fig. 5B) and G)).

The FE-SEM images were used to evaluate the success of incorporating the metal dopants into the bioceramic structure.

In Fig. 5E)–G), hydroxyapatite coatings with the three metal dopants copper, silver and bismuth are shown. A distinctive secondary phase that is precipitated between the splats can be observed, especially for the silver doped coatings (Fig. 5E) and H)). These silver precipitates are an order of magnitude smaller than the particles of the bioceramic matrix and can be distinguished from the bioceramic by the use of backscattered electrons, through which the silver with the higher atomic number appears brighter than the calcium phosphate. In Fig. 5H), a 20,000× magnification of a silver-doped TCP coating shows that the silver precipitates between the TCP-splats with particle sizes in the submicron range down to 100 nm. The bismuth in Fig. 5F) also shows precipitates in the submicron range on the surface of the coating.

The copper doped coating in Fig. 5G) shows some precipitates on the surface structures. These precipitates however are not as distinctive as the silver precipitates and could also not be differentiated as clearly through the use of backscattered electrons as the silver, probably due to the lower atomic weight of copper.

For a better identification of the copper in the coating, an EDX mapping on a polished cross-section of a copper doped hydroxyapatite coating was performed (Fig. 6). In the reference image for the element mapping as well as the weight distribution of calcium, copper and oxygen is depicted. The brighter spots in the reference image correspond well with the spots of concentrated copper. For the bigger spots with a size of about 300 nm, the copper particle also corresponds with a lack of oxygen, which indicates the occurrence of metallic copper. Due to the limited resolution of the element mapping, it is not possible to distinguish between metallic copper and copper oxides for very small particles. The copper signal can be detected in all areas of the cross section, indicating that the precipitation of copper during thermal spraying results in a distribution of the copper particles throughout the coating. While it is possible that there is a concentration of metal particles in certain areas (for example on the surface) of the deposited layer, the deposition of the coating in multiple layers due to the multiple torch passes, should ensure that the metal particles are evenly distributed in the coating.

This method of deposition of metal phases is possible through carefully adjusted process parameters such as a non-stochiometric oxygen-to-ethene ratio and the optimum spraying distance. However, due to the high temperatures during the coating process, the dopant does not occur as a pure metal phase. In case of copper, a mixture of copper as well as copper oxide (cuprite and tenorite) is deposited.

3.2. Phase analysis

The phase compositions of the coatings were evaluated using X-ray diffraction (Fig. 7). The hydroxyapatite and the GB14 implant

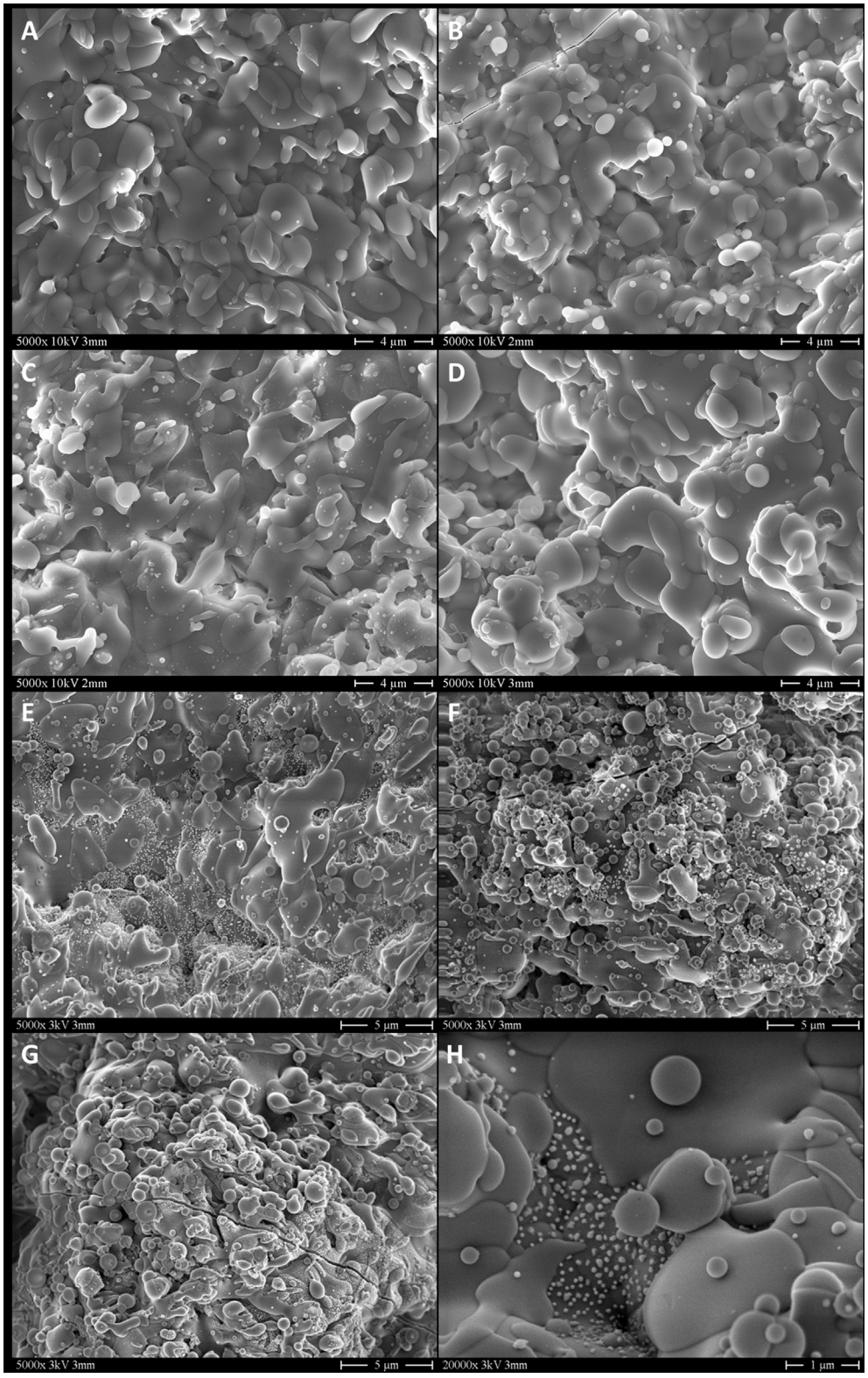

Fig. 5. SEM images of the coating surfaces: A) HA; B) TCP; C) GB14; D) bioglass; E) HA with silver; F) HA with bismuth; G) HA with copper; H) TCP with silver.

coating correspond well to their respective spray powders. It appears that no significant amount of thermal decomposition occurs during the spraying process which could result in the formation of other calcium phosphate phases or compounds.

The diffractogram of the TCP however shows a change in phase composition from the starting powder to the implant coating. This change in phase composition is probably due to the heating and melting of the material during the thermal spray process, resulting in a mixture of α- and β-TCP as well as other phases in the final implant coating. Due to the amorphous nature of the bioglass, the

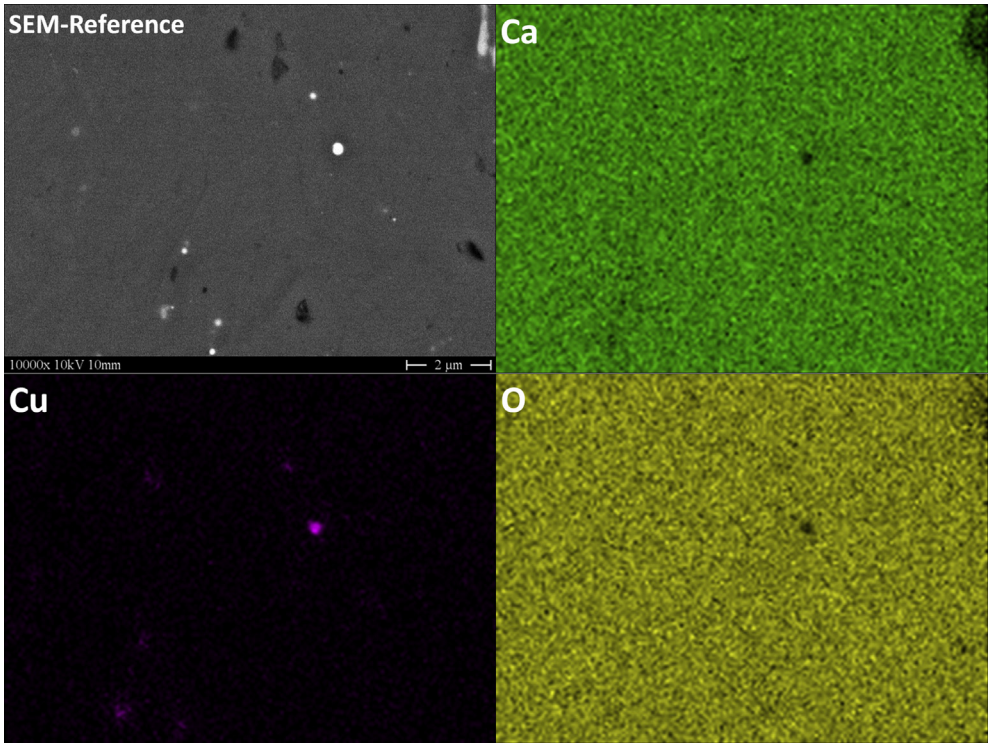

Fig. 6. EDX mapping of a copper doped hydroxyapatite cross-section.

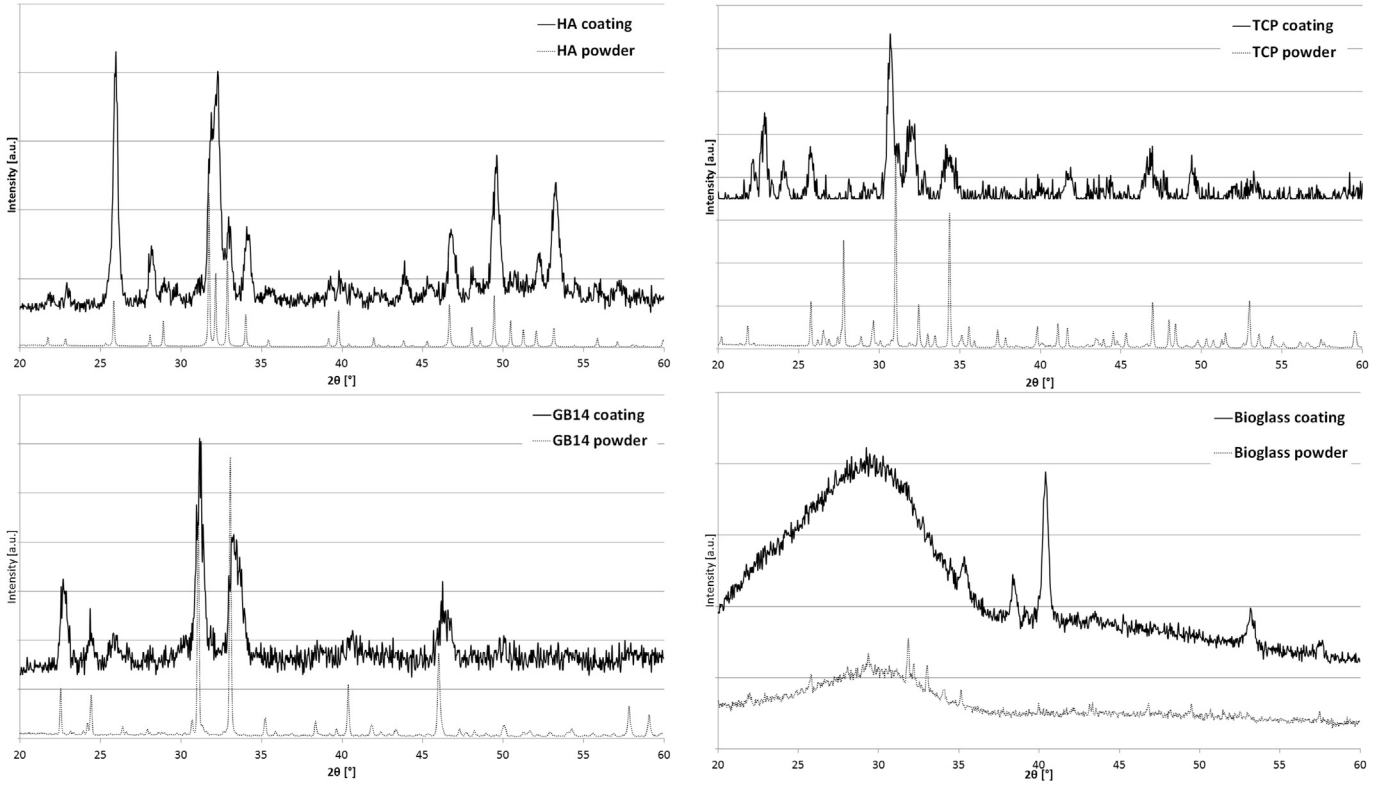

Fig. 7. X-ray diffraction of all bioceramic coatings. Respective patterns of spray powders are shown for comparison.

diffractograms of the powder and the coating are quite similar with the exception of the peaks that correspond to the titanium substrates. Because the coating thickness of the suspension flame sprayed coatings is comparable to the penetration depth of the X-ray, and since the bioglass coating are marginally thinner than the other bioceramic coatings, the titanium substrate was measured as

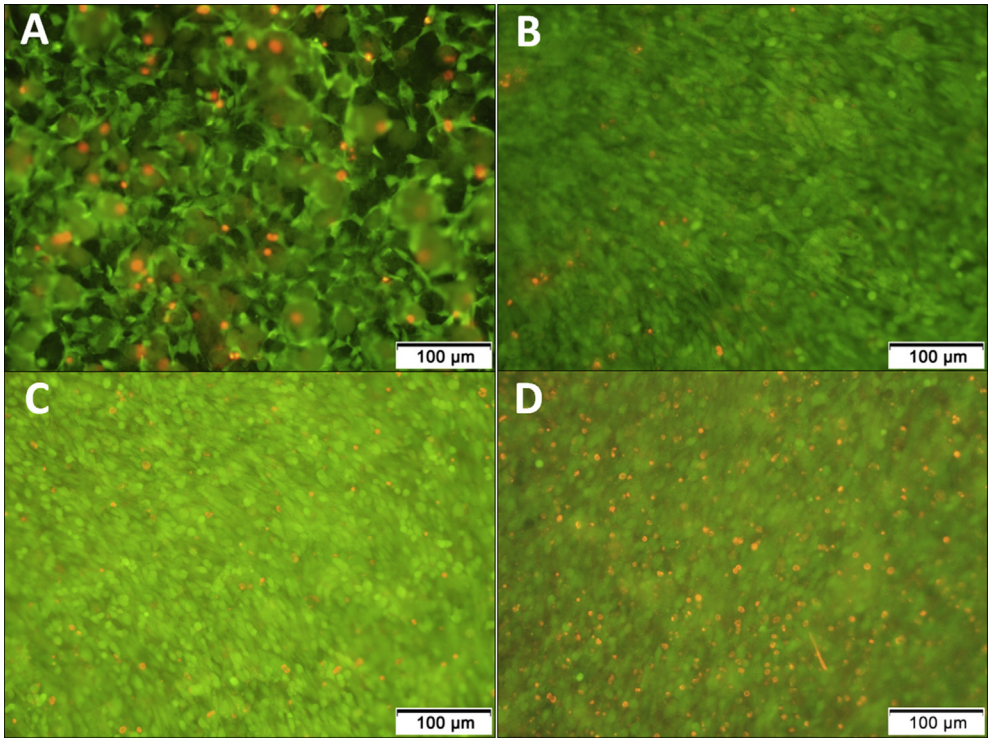

Fig. 8. Live/dead-assay on TCP coating with silver after A) three days; B) seven days; C) 14 days; D) 21 days. Green: living cells; red: dead cells.

well as the coating.

3.3. Biocompatibility

The live/dead-assay, as shown in Fig. 8 for a TCP coating with silver, was performed on all material systems to evaluate the cell viability after three, seven, 14 and 21 days. While there are some dead cells (red), the vast majority are vital cells (green). After seven days, the cells form a confluent layer.

In Fig. 9, an overview of the viability of the cells on all materials is shown. The cell compatibility of the coatings is quite different in the beginning. The cell viability on the HA coatings is lower than the other material systems at day 3 and 7.

This difference could be caused by the different solubility of the bioceramic materials, resulting in a slower or faster degradation of the coatings. However, after 21 days almost all coatings show comparable cell viability. No cell toxicity caused by the metal dopants was observed.

4. Conclusions

Thermal spraying with suspensions offers new possibilities in

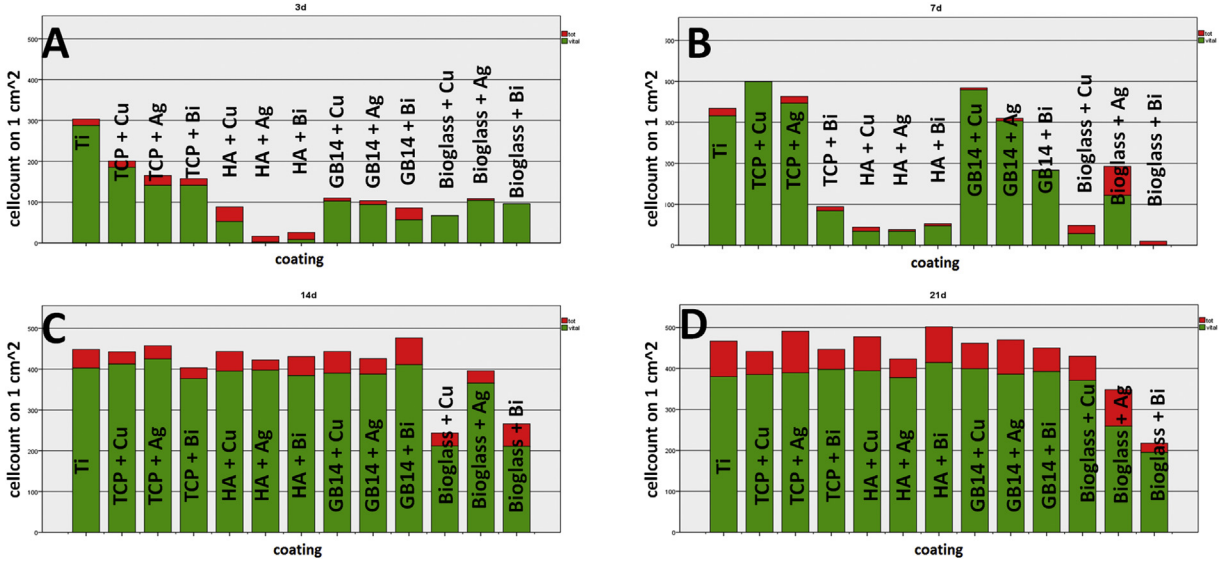

Fig. 9. Live/dead-assay on all coatings: ratio of vital cells after A) 3 days; B) 7 days; C) 14 days; D) 21 days.

regard to coating composition and properties. The combination of bioceramic suspension with metals or metal precursors results in a dispersed secondary phase in a bioceramic matrix. In this study, four different bioceramic materials were combined with different metals with known antibacterial properties in order to evaluate their potential as implant coatings that offer good biocompatibility as well as infection prophylaxis.

Especially soluble copper and silver salts offer an interesting approach for the manufacturing of these coatings due to their rather simple and reliable integration in the suspension formulation and the spraying process. By adjusting the process parameters, a suitable processing window for the combination of bioceramic matrix and metal dopant was established: the different bioceramic matrix materials show a phase composition comparable to the starting powders and a suitable crystallinity whereas the metal dopants were deposited as a mixture of metallic material as well as oxide phases. The evaporation of the liquid phase of the suspension in the combustion chamber and the subsequent precipitation of the metal particles result in a fine distribution of particles in the coatings.

While the oxidation of the metals can be controlled to a certain extent through the oxygen-ethene-mixture, torch configuration and torch kinematic, a certain amount of oxidation appears to be inevitable given the necessity of keeping the spraying parameters also suitable for the bioceramic material.

The evaluation of the biocompatibility suggests that the concentration of metal is suitable, so that the coatings show no cell toxicity. Further in vitro as well as in vivo test will focus on the biocompatibility, the release of metals and the antibacterial behavior.

Acknowledgments

The authors would like to thank the Deutsche Forschungsgemeinschaft DFG for the funding of this work under grant GA 589/11-1 and BE 1964/8-1. We thank G. Maier from Max Planck Institute for Intelligent Systems, Stuttgart, for his assistance with the XRD measurements.

References

[1] Betty Leon, John A. Jansen, Thin Calcium Phosphate Coatings for Medical Implants, 2009.
[2] S. Kurtz, K. Ong, E. Lau, F. Mowat, M. Halpern, Projections of primary and revision hip and knee arthroplasty in the United States from 2005 to 2030, J. Bone Jt. Surg. Am. 89 (4) (2007) 780–785.
[3] W. Zimmerli, Bone and Joint Infections: from Microbiology to Diagnostics and Treatment, Wiley, Hoboken, 2014.
[4] S. Aslam, R.O. Darouiche, Prosthetic joint infections, Curr. Infect. Dis. Rep. 14 (5) (2012) 551–557.
[5] S.M. Kurtz, E. Lau, J. Schmier, K.L. Ong, K. Zhao, J. Parvizi, Infection burden for hip and knee arthroplasty in the United States, J. Arthroplasty 23 (7) (2008) 984–991.
[6] Y. Chen, X. Zheng, Y. Xie, C. Ding, H. Ruan, C. Fan, Anti-bacterial and cytotoxic properties of plasma sprayed silver-containing HA coatings, J. Mater. Sci. Mater. Med. 19 (12) (2008) 3603–3609.
[7] Q. Ling Feng, T. Nam Kim, J. Wu, E. Seo Park, J. Ock Kim, D. Young Lim, F. Zhai Cui, Antibacterial effects of Ag-HAp thin films on alumina substrates, Thin Solid Films 335 (1–2) (1998) 214–219.
[8] J.L. Clement, P.S. Jarrett, Antibacterial silver, Metal-based Drugs 1 (5–6) (1994) 467–482.
[9] D.-J. Lin, M.-T. Tsai, T.-M. Shieh, H.-L. Huang, J.-T. Hsu, Y.-C. Ko, L.-J. Fuh, In vitro antibacterial activity and cytocompatibility of bismuth doped micro-arc oxidized titanium, J. Biomater. Appl. 27 (5) (2013) 553–563.
[10] J. O'Gorman, H. Humphreys, Application of copper to prevent and control infection. Where are we now? J. Hosp. Infect. 81 (4) (2012) 217–223.
[11] Y.Z. Wan, G.Y. Xiong, H. Liang, S. Raman, F. He, Y. Huang, Modification of medical metals by ion implantation of copper, Appl. Surf. Sci. 253 (24) (2007) 9426–9429.
[12] G. Bolelli, D. Bellucci, V. Cannillo, R. Gadow, A. Killinger, L. Lusvarghi, P. Müller, A. Sola, Comparison between suspension plasma sprayed and high velocity suspension flame sprayed bioactive coatings, Surf. Coat. Technol. 280 (2015) 232–249.
[13] G. Bolelli, V. Cannillo, R. Gadow, A. Killinger, L. Lusvarghi, A. Sola, N. Stiegler, Microstructure and in-vitro behaviour of a novel high velocity suspension flame sprayed (HVSFS) bioactive glass coating, Surf. Coat. Technol. 205 (4) (2010) 1145–1149.
[14] G. Bolelli, V. Cannillo, R. Gadow, A. Killinger, L. Lusvarghi, J. Rauch, Microstructural and in vitro characterisation of high-velocity suspension flame sprayed (HVSFS) bioactive glass coatings, J. Eur. Ceram. Soc. 29 (11) (2009) 2249–2257.
[15] L. Altomare, D. Bellucci, G. Bolelli, B. Bonferroni, V. Cannillo, L. de Nardo, R. Gadow, A. Killinger, L. Lusvarghi, A. Sola, N. Stiegler, Microstructure and in vitro behaviour of 45S5 bioglass coatings deposited by high velocity suspension flame spraying (HVSFS), J. Mater. Sci. Mater. Med. 22 (5) (2011) 1303–1319.
[16] L.A. Díaz, B. Cabal, C. Prado, J.S. Moya, R. Torrecillas, A. Fernández, I. Arhire, P. Krieg, A. Killinger, R. Gadow, High-velocity suspension flame sprayed (HVSFS) soda-lime glass coating on titanium substrate: its bactericidal behaviour, J. Eur. Ceram. Soc. 36 (10) (2016) 2653–2658.
[17] A.K. Lynn, D.L. DuQuesnay, Hydroxyapatite-coated Ti–6Al–4V: hydroxyapatite-coated Ti–6Al–4V: Part 1: the effect of coating thickness on mechanical fatigue behaviour, Biomaterials 23 (9) (2002) 1937–1946.
[18] P.L. Fauchais, J.V. Heberlein, M.I. Boulos, Thermal Spray Fundamentals: from Powder to Part, Springer US, Boston, MA, s.l., 2014.
[19] R.B. Heimann, Thermal spraying of biomaterials, Surf. Coat. Technol. 201 (5) (2006) 2012–2019.
[20] A. Cattini, D. Bellucci, A. Sola, L. Pawłowski, V. Cannillo, Suspension plasma spraying of optimised functionally graded coatings of bioactive glass/hydroxyapatite, Surf. Coat. Technol. 236 (2013) 118–126.
[21] A. Cattini, D. Bellucci, A. Sola, L. Pawłowski, V. Cannillo, Functional bioactive glass topcoats on hydroxyapatite coatings: analysis of microstructure and in-vitro bioactivity, Surf. Coat. Technol. 240 (2014) 110–117.
[22] R.B. Heimann, Plasma-sprayed hydroxylapatite-based coatings: chemical, mechanical, microstructural, and biomedical properties, J. Therm. Spray. Tech. 25 (5) (2016) 827–850.
[23] R. Gadow, A. Killinger, N. Stiegler, Hydroxyapatite coatings for biomedical applications deposited by different thermal spray techniques, Surf. Coat. Technol. 205 (4) (2010) 1157–1164.
[24] N. Stiegler, D. Bellucci, G. Bolelli, V. Cannillo, R. Gadow, A. Killinger, L. Lusvarghi, A. Sola, High-velocity suspension flame sprayed (HVSFS) hydroxyapatite coatings for biomedical applications, J. Therm. Spray. Tech. 21 (2) (2012) 275–287.
[25] R. Gildenhaar, G. Berger, E. Lehmann, C. Knabe, Development of alkali containing calcium phosphate cements, KEM 361–363 (2008) 331–334.
[26] A. Killinger, P. Müller, R. Gadow, What do we know, what are the current limitations of suspension HVOF spraying? J. Therm. Spray. Tech. 24 (7) (2015) 1130–1142.